Journal of Physics: Conference Series **443** (2013) 012057 doi:10.1088/1742-6596/443/1/012057

Account of the intratrack radiolytic processes for interpretation of the AMOC spectrum of liquid water

D S Zvezhinskiy[1], M Butterling[2], A Wagner[2], R Krause-Rehberg[3] and S V Stepanov[1]

[1] Institute for Theoretical and Experimental Physics, B. Cheremushkinskaya, 25, Moscow, 117218, Russia
[2] Institute of Radiation Physics, Helmholtz-Zentrum, Dresden-Rossendorf, P.O. Box 510119, Dresden, 01314, Germany
[3] Martin-Luther-University Halle-Wittenberg, Dept. of Physics, Halle, 06099, Germany

E-mail: zmitja@yandex.ru

Abstract. Recent development of the Gamma-induced Positron Spectroscopy (GiPS) setup significantly extends applicability of the Age-Momentum Correlation technique (AMOC) for studies of the bulk samples. It also provides many advantages comparing with conventional positron annihilation experiments in liquids, such as extremely low annihilation fraction in vessel walls, absence of a positron source and positron annihilations in it. We have developed a new approach for processing and interpretation of the AMOC-GiPS data based on the diffusion recombination model of the intratrack radiolytic processes. This approach is verified in case of liquid water, which is considered as a reference medium in the positron and positronium chemistry.

1. Introduction

The important step towards further development of AMOC was made by adopting an electron LINAC to produce positrons inside an investigated sample with the help of bremsstrahlung [1]. This experimental method is known as Gamma-induced Positron Spectroscopy (GiPS). The absence of a conventional positron source makes possible to produce positrons over the whole volume of an investigated medium. This might be potentially useful for easier treatment of biological and chemical samples of solid and liquid state.

Before starting various physico-chemical investigations on GiPS setup, we have decided to measure AMOC spectrum of liquid water, which is usually considered as a reference medium for positron studies. Available experimental data for water [2, 3] may provide good quantitative comparison of lifetime and Doppler parameters obtained by novel AMOC-GiPS setup.

2. Theoretical model for AMOC spectrum

Importance of taking into account the radiolytic processes for interpretation of annihilation lifetime spectra was demonstrated in [4]. In the present work we generalize this model to apply for AMOC data. We have attributed some energy distribution for annihilation gamma-quanta produced from different positron states participating in intratrack radiolytic reactions. Further details concerning the diffusion-recombination model can be found in [5, 4].


Content from this work may be used under the terms of the Creative Commons Attribution 3.0 licence. Any further distribution of this work must maintain attribution to the author(s) and the title of the work, journal citation and DOI.
Published under licence by IOP Publishing Ltd

Energy distributions of annihilation radiation, which correspond to certain positron states, are usually described by the Gaussian functions centered at 511 keV energy [6].

In present work we use the same approximation except for the shape of the "narrow" (p-Ps) component, which is calculated according to the so-called finite well Ps bubble model. This model yields positronium annihilation rates as well [7]. Being linked to the energy dimension, it allows to reduce overall number of the adjustable parameters. The lifetime and energy shape of p-Ps AMOC relief depend on the radius R of the Ps bubble state and depth U of the potential well (or on electron penetration depth δ) [8].

Shape of the Doppler spectrum, that is a distribution of annihilation gammas on their energy, is given by the following expression:

$$C(\Delta) \sim \int \rho(\mathbf{p}) \cdot \delta\left(\Delta - \frac{cp}{2}\cos\theta\right) \frac{d^3p}{(2\pi\hbar)^3}. \tag{1}$$

Here $\rho(\mathbf{p})$ is the momentum distribution of the positron-electron pair, Δ is the difference between the energy of annihilating photon and mc^2 =511 keV and θ is the angle between $\mathbf{p}$ and direction to the energy detector. In the spherically symmetrical case $\rho(\mathbf{p}) = \rho(p)$ after integration over θ Eq.(1) is reduced to a simpler form:

$$C(\Delta) \sim \int_{2|\Delta|/c}^{\infty} p\rho(p)dp. \tag{2}$$

Expression for $\rho(k) = \rho(p/\hbar)$ can be calculated by taking Fourier transformation from the wave-function of the point-like Ps, which is given by the finite well Ps bubble model (e.g. see [8] for the description of calculation procedure):

$$\rho(k) \sim \left[\frac{1}{k_U^2 - k^2}\left(\sin k_U R_U \cos kR_U - \frac{k_U}{k}\cos k_U R_U \sin kR_U\right) + \frac{\sin k_U R_U}{k^2 + \kappa^2}\left(\cos kR_U + \frac{\kappa}{k}\sin kR_U\right)\right]^2. \tag{3}$$

Here $\kappa = -k_U/\tan(k_U R_U)$, $k_U = \frac{\sqrt{2E_{\mathrm{Ps}}/Ry}}{a_0}$, a_0 is the Bohr radius (=0.53 Å), Ry=13.6 eV, E_{Ps} is the energy of Ps inside the finite well with radius R_U and depth U.

Substitution of Eq.(3) into Eq.(2) gives theoretical shape of the Doppler line for p-Ps. For fitting of the experimental data it must be convolved with the energy resolution function.

2.1. Background events

The model of background does not contain the Compton plateau, which is usually produced by annihilation gammas below 511 keV. This effect is significantly reduced with BGO escape-supression shields attached to HP-Ge energy detectors [9]. Though the Compton scattered gammas are observed, they result in negligible difference between low- and high-energy tails of spectrum.

Let us review the reason for appearance of background events in GiPS-AMOC experiment (see Fig. 1). Prompt gammas give birth to the positron. Though energy of bremsstrahlung, which enters the sample chamber, has mainly an order of some MeV, its scattered fraction is able to trigger energy detector by releasing the energy of ~511 keV in it. On the other hand, the positron (and positronium) appeared in the sample produces annihilation gammas, one of which may trigger the time detector. Such a mixture of true (annihilation) and false (caused by scattered bremsstrahlung) events recorded by age and energy detectors correspondingly gives rise to the relief of background events

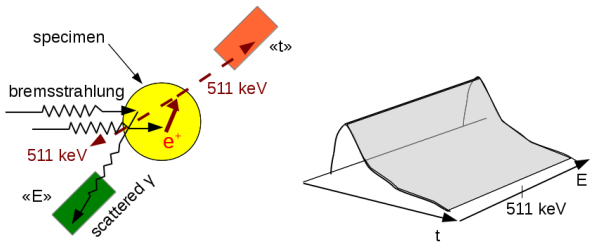

Figure 1. Appearance of background events

shown in Fig. 1. Thus the projection of background component on the time axis is similar to the lifetime spectrum of the investigated medium and its energy projection is constant.

We have taken into account an appearance of the "reversed" events, which come from detection true annihilation events (one of the annihilation gammas is detected by the energy detector, while scattered bremsstrahlung triggers the time detector). However, overall contribution of these events to the observed spectrum, turned out to be quite small.

2.2. Time and energy resolution function

The time resolution function is important for the spectrum processing. Usually it is fixed from independent experiments done with the reference samples such as annealed Fe, monocrystalline Si, kapton etc.

In GiPS, parameters of the temporal resolution function may depend on the investigated medium along with the sample dimensions. Distinct spatial distribution of annihilation events, which depends on positron birth rate in a certain medium, leads to variation of the parameters of the resolution function (e.g. its FWHM varies from 180 ps in Fe sample to 215 ps in water). Therefore, dispersion of the resolution function is accepted as ajustable parameter in our model.

The energy resolution function was measured with a help of ^{137}Cs and ^{60}Co isotopes. Then it was extrapolated to 511 keV energy region. We fixed its FWHM on 1.52 keV value.

3. Experimental data processing

3.1. Gauss-exponential decomposition

The AMOC spectrum of twice distilled water was measured at room temperature. Water was poured to the kapton tube. The oxygen removal was made by bubbling nitrogen through the sample before the measurement. The spectrum contains $\sim 4.5\times10^6$ events, which required a week of measurement session. Energy range of annihilation radiation acquired to the spectrum is from 501 to 520 keV.

We have used the ROOT framework [11] to fit theoretical models to the experimental data. The fitting strategy was the following.

To compare the data with the previous experimental data [3, 2], we have decomposed it into a set of the simplest gauss-exponential functions $h_i(E,t) = g_i(E) \cdot f_i(t)$, where $g_i \sim \exp(-\frac{(E-511\text{ keV})^2}{2\sigma_i^2})$ describes the energy distributions of the annihilation gammas. Age distribution functions, f_i, were taken in the form of exponents: $f_i(t) \sim \exp(-t/\tau_i)$.

Data decomposition was made into three h_i functions (p-Ps, positron and o-Ps states) and the background contribution by means of maximization of the likelihood function. We have obtained that "narrow" energy data interval used for fitting yields smaller dispersion of the p-Ps component (Tab. 1). Anyway the results agree well with the literature data [2, 3].

Table 1. Fitting of the water GiPS-AMOC spectrum with a help of the "gauss-exponential" model with the fixed $I_3/I_1 = 3/1$ ratio.

	Full E range			E= 506.5...515.5 keV		
	Intensity	τ, ns	σ, keV	Intensity	τ, ns	σ, keV
o-Ps	0.260(1)	1.767(3)	1.053(2)	0.257(1)	1.788(3)	1.034(2)
e^+	0.653	0.357(1)	1.146(1)	0.657	0.368(1)	1.097(1)
p-Ps	0.087	0.187(2)	0.209(10)	0.086	0.178(2)	0.346(10)

The reason of such a behavior may be more complicated shape of the energy background projection (it could be not a flat one, but of parabolic or gaussian shape), which is neglected in

Table 2. Parameters of the Ps bubble and the diffusion-recombination model obtained from the experimental data fitting in the narrow energy range (506.5...515.5 keV). Uncertainties were estimated as the differences between adjustable parameters obtained for the narrow and full energy ranges

Par.	R, Å	R_{ox}=R_{opc}, Å	σ_{e^+}, keV	σ_{o-Ps}, keV	τ_{e^+}, ns	δ, Å	η
Value	3.4(2)	5.8(6)	1.20(1)	1.04(12)	0.31(2)	0.85(1)	0.74(20)

the present fitting.

3.2. Diffusion-recombination model

To reduce a number of free parameters at fitting the data with more complicated theoretical model, we have fixed parameters of the time resolution function and the background, which were obtained from the gauss-exponential decomposition. Table 2 summarizes the obtained results.

The set of parameters yielded by the diffusion-recombination model agree well with the previously reported values [4]. The value of δ, also called as "electron penetration depth", is lesser than reported previously from conventional lifetime spectra [4], which means higher value of corresponding potential well depth (U$\sim$6 eV). The relative contact density parameter, η, also agrees well with the results known from the magnetic quenching experiment [12], though its estimated variability implies that it should be fixed. Both energy and time resolution functions were fixed to that obtained from the gauss-exponential decomposition. In the fitting we also assumed that the oxidation reaction radius R_{ox} equals to the ortho-para conversion reaction radius R_{opc}. Within the present model this radius should be considered as an averaged reaction characteristic for Ps bubble state over all oxidizers (OH radical, H_3O^+) and ortho-para convertors (OH, H, radical-cation H_2O^+, hydrated electron).

4. Summary

Annihilation spectrum measured in water by means of GiPS-AMOC setup is consistent with previously reported results. Its convetional (gauss-exponential) decomposition does not show any deviations from the known values.

Our attempt to describe this spectrum with a help of the diffusion-recombination model shows that the model is also consistent with the measured spectrum and parameters of the model are in agreement with previously reported values [4].

References

[1] Butterling M et al. 2011 *NIM B* **269** p 2623
[2] Mogensen O E 1995 *Positron annihilation in chemistry* (Springer-Verlag)
[3] Castellaz P et al. 2002 *J. Nucl. Radiochem. Sci.* **3 (2)** p R1
[4] Stepanov S V et al. 2011 *Mat. Sci. Forum* **666** p 109
[5] Stepanov S V and Byakov V M 2005 *High Energy Chemistry* **39 (3)** p 131; *High Energy Chemistry* **39 (5)** p 282
[6] Castellaz P et al. 1996 *J.Radioanal.Nucl.Chem.* **210(2)** p 457
[7] Byakov V M and Stepanov S V 2000 *Rad.Phys.Chem.* **58** p 687
[8] Stewart A T, Briscoe C V and Steinbacher J J 1990 *Can. J. Phys* **68** p 1362
[9] Schwengner R et al. 2005 *NIM A* **555 (1-2)** p 211
[10] http://kinetics.nist.gov/solution/
[11] Brun R, Rademakers F 1997 *Proc. AIHENP'96 Workshop* **389** p 81, `http://root.cern.ch`
[12] Bisi A, Consolati G, Gambarini G and Zappa L 1985 *Nuovo Cimento* **5D** p 358